energies

MDPI

Article

In-Situ Efficiency Estimation of Induction Motors Based on Quantum Particle Swarm Optimization-Trust Region Algorithm (QPSO-TRA)

Mahamadou Negue Diarra, Yifan Yao, Zhaoxuan Li, Mouhamed Niasse, Yonggang Li and Haisen Zhao *

School of Electrical and Electronic Engineering, North China Electric Power University, Beijing 102206, China; diarraneguess82@yahoo.fr (M.N.D.); yaoyifan2000@ncepu.edu.cn (Y.Y.); 120202201393@ncepu.edu.cn (Z.L.); mhniasse@ncepu.edu.cn (M.N.); 51350586@ncepu.edu.cn (Y.L.)
* Correspondence: zhaohisen@ncepu.edu.cn

Abstract: The accuracy estimation of induction motors' efficiency is beneficial and crucial in the industry for energy savings. The requirement for in situ machine efficiency estimation techniques is increasing in importance because it is the precondition to making the energy-saving scheme. Currently, the torque and speed identification method is widely applied in online efficiency estimation for motor systems. However, the higher precision parameters, such as stator resistance R_s and equivalent resistance of iron losses R_{fe}, which are the key to the efficiency estimation process with the air gap torque method, are of cardinal importance in the estimation process. Moreover, the computation burden is also a severe problem for the real-time data process. To solve these problems, as for the torque and speed-identification-based efficiency estimation method, this paper presents a lower time burden method based on Quantum Particle Swarm Optimization-Trust Region Algorithm (QPSO-TRA). The contribution of the proposed method is to transform the disadvantages of former algorithms to develop a reliable hybrid algorithm to identify the crucial parameters, namely, R_s and R_{fe}. Sensorless speed identification based on the rotor slot harmonic frequency (RSHF) method is adopted for speed determination. This hybrid algorithm reduces the computation burden by about 1/3 compared to the classical genetic algorithm (GA). The proposed method was validated by testing a 5.5 kW motor in the laboratory and a 10 MW induction motor in the field.

Keywords: in situ efficiency; induction motors; quantum particle swarm optimization; trust region algorithm; QPSO-TRA; rotor slot harmonics frequencies

Citation: Diarra, M.N.; Yao, Y.; Li, Z.; Niasse, M.; Li, Y.; Zhao, H. In-Situ Efficiency Estimation of Induction Motors Based on Quantum Particle Swarm Optimization-Trust Region Algorithm (QPSO-TRA). *Energies* **2022**, *15*, 4905. https://doi.org/10.3390/en15134905

Academic Editor: Armando Pires

Received: 27 May 2022
Accepted: 28 June 2022
Published: 5 July 2022

1. Introduction

The increasing demand for energy combined with rising energy costs has led to a desire to increase energy utilization efficiency. Induction motors (IMs) are the most commonly used motors in the industry. They are essential components in the chains of drive systems. The efficiency estimation strategies of all induction motors require good knowledge of the machine parameters to ensure an accurate estimation. The problem of estimating the parameters of induction motors and their efficiency is considered the most critical and complex matter in industries, in in situ situations. However, the higher accuracy of IM parameters is of capital importance in all industrial processes since it directly affects the performance of the control systems. One of the main reasons for monitoring a motor's efficiency is to ensure that energy conversion occurs with the least energy supply. Another reason is that the nominal parameters obtained from manufacturers might not be the same as those under actual motor operating conditions. This is due to several factors such as aging, rewinding, and voltage unbalance. Hence, it is necessary to estimate these parameters in in situ for any in situ induction motors efficiency estimation. As for the speed, it can be affected by bearing faults. Estimating the speed in in situ has several advantages. It can be used to check bearing faults and motor efficiency estimation online.

Therefore, estimating induction motors' parameters and speed in in situ can be helpful for all industrialists because it can give information about the motors' healthy state and avoid extra cost for speed measuring devices. While effort is being made to design and manufacture more efficient induction motors (IMs), monitoring a machine's operational efficiency helps reduce energy costs by ensuring that it is running in its optimal efficiency range. Numerous works have been published for estimating the efficiency of the electrical machines in situ, under the loaded condition without disturbing their operation [1,2]. To assess energy efficiency and enhance the overall performance of the industrial processes, it is essential to identify energy loss and monitor the efficiency in real time [3].

Generally, torque and speed measurements are made to estimate the induction motor's efficiency. However, if an efficiency estimation of an induction motor is required for an in situ situation, whose operation cannot be disrupted because of the ongoing critical industrial process, torque determination becomes problematic.

The procedure of determining the parameters of an induction motor is well-known for estimating efficiency. The parameters of the induction motor's per-phase equivalent model can be determined by the no-load and locked rotor test or the IEEE Standard 112 impedance test method. No-load and locked rotor tests are not practicable in in situ [4,5]. In in situ situations, the Genetic Algorithm (GA) is mainly used for parameter identification, demanding more central processing unit (CPU) and computational time [6]. To sum up, the methods for efficiency estimation can be categorized as follows.

(1) Slip methods;
(2) Current methods;
(3) Segregated loss method;
(4) Equivalent circuit-based method;
(5) Nonintrusive air gap torque (NAGT) methods;
(6) Air gap torque (AGT) methods;
(7) Shaft torque method.

Among the above methods, each of the following methods for efficiency estimation has its advantages and disadvantages according to the application domain. Some of them cannot be employed for in situ efficiency estimation. However, the current and slip methods are straightforward and nonintrusive, but they are lacking in high accuracy [7], which is unsuitable for any efficiency assessment. Despite having very high precision, the segregated loss method [8] is intrusive for use in in situ conditions. To limit the intrusiveness, empirical results are used, which could diminish the accuracy of those procedures [9]. The equivalent circuit method requires no-load and locked rotor tests or variable voltages and frequency supplies, making them unsuitable for in situ applications. The air-gap torque (AGT) and the shaft torque method consider harmonic distortion because it uses the operating voltage and current signals to calculate this torque [10], which makes it appreciable for in situ efficiency estimation.

The most challenging task in efficiency estimation is the determination of the output power. The online efficiency estimation method can be classified into the equivalent circuit and the torque and speed methods from the above analysis. The first method must determine all the losses and subtract them from the input power. The second one must determine the shaft torque through the air gap torque, and the speed is estimated as described in Section 2.1 to determine the output power. For the second method, the core losses resistance R_{fe} and the stator resistance R_s must first be identified online for air gap torque calculation, these are dependent on the operating condition. Furthermore, the problem in the current identification method of these parameters is that the time and the computation burden of the algorithm used are high enough, or the algorithm used for parameters identification is not accurate enough. The AGT and the shaft torque method are adopted in this paper to calculate the output power.

The contribution of this paper is firstly to propose a new algorithm to identify the motor parameters simultaneously. The computation time and burden can be reduced significantly since the global search is avoided. In the presented method, a hybrid algorithm

derived from PSO and TRA is used, the Quantum Particle Swarm Optimization-Trust Region Algorithm QPSO-TRA, to improve the deficiencies of PSO and TRA. The time burden of the proposed hybrid QPSO-TRA is slightly larger than that of the standard PSO, but the identification is more accurate than the standard PSO.

2. Efficiency Estimation Method

This study adopts an efficiency estimation method based on torque and speed identification. The output torque and rotor speed should first be determined by air gap torque and rotor slot harmonic methods [11]. Then, the output power P_2 can be obtained. The input power P_1 is calculated by measured current and voltage. Finally, efficiency can be calculated by P_2/P_1. To obtain P_2, several processes are involved, which have to be accurately investigated to avoid calculation mistakes.

2.1. Torque and Speed Determination Methods

During the operation of the induction motors, despite many internal excitations that can rise to system complexity, the external environment, such as unsymmetrical voltage sags or external load variation, can also be unstable, etc. The electromechanical behavior of an induction motors change according to the actual load changes from the start-up no-load to the full-load condition. In addition, considering that the electromechanical power is the transmitted power from the stator to the rotor through the air gap, it includes the actual load effect since it depends on the actual current and voltage and the core loss power P_{fe} as can be seen in (2) because the motors' running current is affected by the load changes. The AGT method was proposed in [12] for in situ efficiency estimation. It is calculated by using the voltage, current, and stator resistance R_s and the core losses P_{fe} data. However, the authors in [12] did not consider the change of the resistance under the operating temperature, which make it unsuitable for real-time calculation. Because of variable current in the winding under different load conditions, the temperature changes affect the motor's winding resistance. The temperature of a machine at the actual loading condition is required to adjust or correct the stator and rotor windings resistances. An initial temperature is determined from the input current at each measured load to overcome this problem, as shown in Equation (1), or directly measured with a temperature sensor. For the best calculation of the air gap torque, the resistance is corrected according to real-time temperature in this study, whereas there is the presence of $R_{s,cor}$ in Equation (2) instead of R_s. The AGT is calculated as in Equation (2).

$$T_{load,Est} = \frac{I_{load}}{I_{rated}}(T_{rated} - T_{ambien}) + T_{ambien} \tag{1}$$

where I_{rated} is the rated load current stated on the machine's nameplate, I_{load} is the actual load current, $T_{load,Est}$ is the actual temperature, T_{ambien} is the ambient temperature, and T_{rated} is the rated load temperature

$$T_{ag} = \frac{p * \sqrt{3}}{6}\{(2 * i_a + i_c) * \int [v_{ca} - R_{s,cor}(i_c - i_a)dt] - (i_b - i_a) * \int [v_{ab} - R_{s,cor}(2 * i_a + i_b)dt]\} - \frac{60P_{fe}}{2\pi n_1} \tag{2}$$

where p is the number of poles; i_a and i_c are line currents; v_{ab} and v_{ca} are line voltages; $R_{s,cor}$ is the stator resistance at the operating temperature, and P_{fe} is the core losses. P_{fe} is calculated using the identified core resistance R_{fe}.

Speed determination is crucial in motors' efficiency estimation. This technique is designed to work without interrupting the industrial process. Measuring the speed of a built IM is a relatively easy task. Still, to measure it, one needs an extra device (speed sensor) which can be expensive and can increase the manufacturing costs for the manufacturer. Therefore, we need to estimate the speed to avoid these additional costs. One phase current is analyzed to extract the rotor harmonics high frequency and then estimate the IM speed. In this method, one does not need to calculate the losses between the input and output power separately to have efficiency. The output power is directly calculated by using the

torque and speed as in (15) and (16). To do so, we need to use $R_{s,cor}$ and R_{fe} in the air gap torque calculation process. This method can avoid extra production costs and considers the motor's temperature change. The different techniques for rotor slot harmonic frequency (RSHF) are summarized below.

An enhanced approach to speed determination utilizing the motor's current harmonics, which arise for stator core form, rotor shaft misalignment, bearing position, and rotor bar resistance variation, was conducted in [13]. The current harmonics can be expressed by Equation (3):

$$f_{sh} = f_1\left[(\lambda Z + n_d)\frac{(1-s)}{p} + \delta\right] \tag{3}$$

where f_{sh} is the current harmonic frequency; f_1 is the supply frequency; $\lambda = 0, 1, 2, 3, \ldots$, Z is the number of rotor slots; $n_d = 0 \pm 1, \ldots$ is the order of rotor eccentricity; s is the slip ratio; p is the number of pole pairs; $\delta = \pm 1, \pm 3, \pm 5$, is the air gap magnetomotive force (MMF) harmonic order.

The fast Fourier transform (FFT) technique successfully improved the speed detection of inverter-fed induction motors via the stator current signal [14]. The generation of rotor slot harmonics (RSHs) in machines is primarily due to the irregular allocation of rotor currents in a finite number of slots as well as the permeance fluctuation in the air gap related to slot opening [15]. In [16], harmonics were used to detect the rotor slot number. It is possible to study the speed and the slip estimation in induction motors using rotor slot harmonics. Thus, the slip can be expressed by Equation (4):

$$s = 1 - \frac{p}{Z}\left(\frac{f_{sh}}{f_1} - \delta\right) \tag{4}$$

From Equation (4), it is possible to determine the rotational speed on the shaft of the induction motor. For that, the expression of the slip is required to be $n = n_s(1 - s)$, where n_s is the synchronous speed and s is the slip; n_s is given by $n_s = 60\,f_1/p$. The rotational speed is thus given by Equation (5):

$$n = \frac{60}{Z}(f_{sh} - \delta f_1) \tag{5}$$

where f_1 is supply frequency, and the rotor slot harmonics frequency f_{sh} is determined by applying digital signal processing techniques.

2.2. Core Losses Determination

Core losses are caused by time-varying magnetic flux. The core losses can be separated into two components, the hysteresis and eddy current effects, as in Equation (6).

$$P_{fe} = P_h + P_e = K_h\omega_e\psi^2 + K_e\omega_e^2\psi^2 \tag{6}$$

where P_h and P_e are the hysteresis and eddy current components of core losses, respectively, Ψ is the stator winding flux linkage, ω_e is the angular frequency, and K_h and K_e are the coefficients of hysteresis and eddy current loss, respectively.

According to Equations (7) and (8), core losses depend only on the angular frequency and the flux linkage if the variation of the coefficients K_h and K_e are neglected. In fact, K_h and K_e rely on the core material's lamination and its thickness. Their variation is slow compared to the angular frequency and flux linkage variation. However, knowing that the core losses are linked to the winding flux linkage and based on the classical electric machine theory, which is assumed to be a sinusoidally varying field, it is evident that the winding flux linkage is proportional to the air gap flux density.

$$P_{fe} = \psi^2(K_h\omega_e + K_e\omega_e^2) \tag{7}$$

$$P_{fe} = \omega_e^2\psi^2/R_{fe} \tag{8}$$

The standard way to determine the core losses is the no-load test. This method is not practicable in the field due to the ongoing production process. After analyzing the above phenomena, this paper proposes a new algorithm to determine the core losses resistance. The core resistance R_{fe} is identified by the new algorithm QPSO-TRA and then uses the voltage to determine the core losses as shown in Equation (9). After R_{fe} identification, this method is robust and straightforward because it considers the voltage fluctuation.

$$P_{core} = 3\frac{V_{ph}^2}{R_{fe}} \tag{9}$$

2.3. Stray Load Loss Determination

According to the IEEE Standard 112-2004 [8], stray load loss at rated load can be assumed, as shown in Table 1.

Table 1. Assumed values for stray load loss [8].

Machines Rating (kW)	Stray Load Loss Percent
1–90	1.8%
91–375	1.5%
376–1850	1.2%
1851 and greater	0.9%

Moreover, it can also be calculated using the International Standard IEC 60034-2-1 [7], as in Equation (10).

$$P_{sll} = P_{in,fl}\left[0.025 - 0.005\log_{10}\left(\frac{P_{out}}{1\text{ kW}}\right)\right] \tag{10}$$

where P_{sll} is the full-load stray load loss, $P_{in,fl}$ is the full-load input power, and P_{out} is the full-load output power.

In [17], a new stray load loss formula has been proposed. It also uses the input power, but it does not use the output power, unlike in Formula (10). The increase in input power due to the unbalance and voltage distortion can be considered. The proposed procedure is, as in Equation (11):

$$P_{sll} = 0.011 * P_{in,fl} \tag{11}$$

where P_{sll} is the stray load loss, and $P_{in,fl}$ is the input power under full-load conditions.

Figure 1 compares three stray load loss determination methods, namely, IEEE method, IEC method, and the improved method in [14]. It is imperative to emphasize that all of the foregoing similarities are only valid if, and only if, the motor under test and the data motor have an identical power rating value. It is found that compared with the tested stray losses, the method in [14] is more accurate. Therefore, this method is adopted to estimate the stray losses in this study.

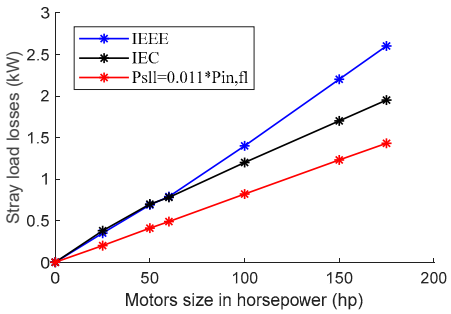

Figure 1. Comparison of three methods of stray load loss determination.

2.4. Friction and Winding (P_{FW}) Losses Determination

An estimation strategy for friction and windage losses has been developed to eliminate this intrusive requirement. This new strategy is based on full-load input power and depends on the motor pole pair number [18], as follows:

(a) If the number of poles is 2, then the friction and windage losses will be calculated using the Equation (12):

$$P_{FW} = 2.5\% * P_{in,fl} \tag{12}$$

(b) If the number of poles is 4, the friction and windage losses will be calculated by Equation (13).

$$P_{FW} = 1.2\% * P_{in,fl} \tag{13}$$

(c) If the number of poles is 6, the friction and windage losses can be calculated by Equation (14).

$$P_{FW} = 1.0\% * P_{in,fl} \tag{14}$$

2.5. Output Torque and Efficiency Determination

From the identified electromagnetic torque, the shaft output torque can be obtained by subtracting stray load loss and friction windage loss as in Equation (15) [19]:

$$T_{shaft} = T_{ag} - \frac{P_{sll} + P_{FW}}{\omega_r} \tag{15}$$

where T_{shaft} is the shaft torque, T_{ag} is the air gap torque, and ω_r is the rotor speed.

Then, output and input power can be calculated by Equations (16) and (17).

$$P_{output} = T_{shaft} * \omega_r \tag{16}$$

$$P_{in} = \sqrt{3} * U * I * \cos\varphi \tag{17}$$

where U is the phase-to-phase voltage, I is the stator current, and cos φ is the power factor.

The motor's efficiency is calculated as in Equation (18).

$$\eta_{est} = \frac{P_{\text{out}}}{P_{\text{in}}} = \frac{T_{\text{shaft}} * \omega_r}{P_{\text{in}}} \tag{18}$$

2.6. Problems in Current Efficiency Determination

The main problem with the above method is accurately identifying the parameters R_s and R_{fe}, which are used in the torque estimation process. In most recent papers, the core loss resistance R_{fe} is ignored, affecting the online efficiency because of the loss caused by this resistance since the AGT will not be accurately determined for the output torque calculation. Several versions of the GA and optimization-based algorithms were used to help to obtain the parameters. The problems of parameters identification technique accuracy are summarized as follows:

(1) R_s and R_{fe} identification with higher precision is vital in all efficiency estimation processes. However, both of them are variants; the first one is a function of the operating condition and the second one is a function of the voltage condition. Therefore, identifying them in real time is essential for efficiency estimation.

(2) A Genetic Algorithm (GA)'s computation time and burden are high. In [4], it is stated that three GAs were constructed to extract the necessary parameters; some versions of GA use binary coding [14], which demands significant time and computational space. The standard PSO is a global search algorithm. Despite having a fast and

straightforward convergence, one of the drawbacks of this algorithm is its global research abilities. If the best particle is a local one in a PSO system, it cannot be accurately identified. In fact, in PSO, the particles will congregate near the global particles if the number of iterations increases.

A new algorithm is proposed to solve these problems. This algorithm does not need to be used three times or coded in binary like some versions of GA, which significantly reduces the computation time and burden, and it is not a global search algorithm. The conception of any optimization algorithm is not a simple task. In this study, the proposed algorithm is more complicated than the standard PSO algorithm in conception and implementation. Still, from the point of view of accuracy, it is better than the standard PSO and some other PSO-based algorithms since it makes full use of the research space. The details of this new algorithm are given in Section 3.

3. Quantum Particles Swarm Optimization-Trust Region Algorithm (QPSO-TRA)

QPSO-TRA is inspired by the PSO algorithm, other PSO-based algorithms, and the TRA algorithm. QPSO-TRA has been inspired by the advantages and disadvantages of some standard former algorithms. It studies the weaknesses of these algorithms and transforms them into benefits for a better investigation of the problems to be solved.

3.1. Standard Particle Swarm Optimization PSO

The mechanism of standard PSO is motivated by the complex social movement shown by biological species such as flocks of birds, schools of fish, swarms of bees, and sometimes social behaviors of the human being. PSO is a relatively simple algorithm and converges fast [20].

In a PSO system, each particle represents a potential solution to the problem and it updates its location by following two optima. One is its personal best location named P_{best}, the best position found by it so far. The other is the global best position P_{gbest}, namely, the best position located by its neighborhood particles so far. The movement of every particle is regulated by the efficacy of its previous location and that of their neighbors. The velocity and the location are formulated as in Equations (19) and (20):

$$v_i(t+1) = \omega * v_i(t) + c_1 * r_1 * (P_{\text{best}_i}(t) - x_i(t)) + c_2 * r_2 * (P_{P_{\text{gbest}_i}}(t) - x_i(t)) \quad (19)$$

$$X_i(t+1) = x_i(t) + v_i(t+1) \quad (20)$$

The inertia weight can be updated by Equation (21):

$$\omega(t) = \omega_{\max} - \frac{t(\omega_{\max} - \omega_{\min})}{iter_{\max}} \quad (21)$$

The velocity value is chosen to be $0.1 \leq k \leq 0.5$ and is set by the user [21]. However, the problem with the PSO algorithm is that it is a global research algorithm. It quickly and easily falls into a local optimum.

3.2. Quantum Particles Swarm Optimization (QPSO)

Inspired by trajectory analysis of the PSO and quantum mechanics, the Quantum Particle Swarm Optimization (QPSO) is an algorithm for problem optimization. The QPSO can find the optimal solution in search space and has the advantage of fewer control parameters, simplicity in software programming, and a relatively fast convergence rate. QPSO is better than standard PSO because, in the standard PSO algorithm, the particles are restricted to a small space for every iteration of the swarm. This restriction will weaken the global search abilities, affect the optimization accuracy, and lead to premature convergence [22]. To improve the search abilities and optimization efficiency and to avoid premature convergence, a quantum is introduced into the PSO. This quantum performs the

mutations of particles to increase the particles' diversity, and their movement is governed by quantum displacement.

The Gaussian sample is based on the personal best position *Pi* and the global personal best position *Pg*. The position of each particle is updated by Equation (22). However, if the global best particle is a local optimum of the problem to be optimized, it is more challenging to break out from this local optimum. Thus, to have a complete and satisfactory use of research space, QPSO must join a local optimal research algorithm such as the "Trust Region Algorithm (TRA)" to enhance its performance.

$$x_{ij} = (t+1) = G\left(\mu_{ij}(t), \sigma_{ij}^2(t)\right) \tag{22}$$

where $x_{ij}(t) = \left(p_{ij}(t) + p_{gj}(t)\right)/2$, $\sigma_{ij}^2(t) = \left|p_{ij}(t) - p_{gj}(t)\right|$ are, respectively, the mean and standard deviation of the Gaussian distribution.

3.3. Trust Region Algorithm (TRA)

TRA is a well-known iterative approach for solving unbounded optimization problems. It uses the method developed by Newton and offers a high degree of convergence and stability [23]. For a given problem, TRA divides the research space into subspaces for a better investigation. At the start, a small region is initialized at each iteration as the trust region centering on the current iteration point. This operation is continuously conducted until all the research space is investigated.

However, multimodal and multivariate problems which necessitate optimization are sometimes trapped in local optima, making it challenging to obtain the optimal global solution. This trap is due to the fact that the following searching direction of TRA is only based on the capacity of the locally developed objective function. Therefore, to overcome this problem, the TRA needs to be associated with a global optimization algorithm.

3.4. Hybrid Algorithm Formed by QPSO and TRA (QPSO-TRA)

Because QPSO is a global optimization algorithm, if the global best particle is a local optimum of the problem to be optimized, it is challenging for QPSO to break out from this local optimum. As for the TRA, it frequently becomes stuck in local optima. A hybrid algorithm is formed by combining QPSO and TRA to avoid the early convergence at the last step of the QPSO algorithm and improve the convergence speed. The advantage of TRA and its research abilities is applied to QPSO. This hybrid algorithm helps to increase or enhance the particle diversity and the global search abilities of the QPSO algorithm. The combined, joined, or hybrid algorithm is then called QPSO-TRA. QPSO-TRA achieves quick and efficient convergence performance at a low computational cost compared to GA. Its computation time is slightly higher than PSO, but it is more accurate than PSO. In the hybrid algorithm, each personal best position is updated according to Equation (23):

$$\begin{cases} p_q(t+1) = x_q(t+1), \\ p_i(t+1) = \begin{cases} p_i(t), fit(p_i(t)) \le fit(x_i(t+1)) \\ x_i(t+1), fit(p_i(t)) > fit(x_i(t+1)) \end{cases} \quad (i \neq q) \end{cases} \tag{23}$$

Let Equation (23) be a function (F) and $\left\{p_g(t)\right\}_{t=0}^{\infty}$ a series or succession generated by the algorithm. Then $\lim_{n\to\infty} P\left(p_g(t)\right) \in R_\varepsilon = 1$, where R_ε is the optimal region, $P\left(p_g(t)\right) \in R_\varepsilon$ is the probability at stage α, and the point $p_g(t)$ generated by the algorithm is in R_ε.

It should be considered that $\left\{p_g(t)\right\}$ is a sequence generated by the QPSO-TRA algorithm, where $p_g(t)$ is the current best position of the swarm on time (t). As the function F is defined as in Equation (24), from the limit, it can be seen that the algorithm converges well.

$$\left\{F(p_g(t), x_i(t)) = \begin{cases} p_g(t), fit\left(p_g(t)\right) \le fit(x_i(t)) \\ x_i(t), fit\left(p_g(t)\right) > fit(x_i(t)) \end{cases}\right. \tag{24}$$

QPSO-TRA satisfies the convergence theories from the above statements, so it is an optimization algorithm. Moreover, from the theorem, QPSO-TRA is an optimum search algorithm that benefits from different algorithms.

The different steps of implementing the algorithm are detailed in Figure 2 and explained in the next section. As constraints, the values of each particle's lower and upper bounds are set. The lower bound (lb) and upper bound (ub) are set for the motor's parameters. One can set as lb = [0.00 0.00 0.00 0.00 0.00 0.00], ub = [2.4.00 1.00 1.20 2853 155.00 5.50] for the six parameters of the motors, namely, stator resistance, stator reactance, rotor reactance, core resistance, magnetizing reactance, and rotor resistance, respectively. The lower and upper bounds depend on the size of the motors. Once the parameters are obtained, they are used in the efficiency estimation process.

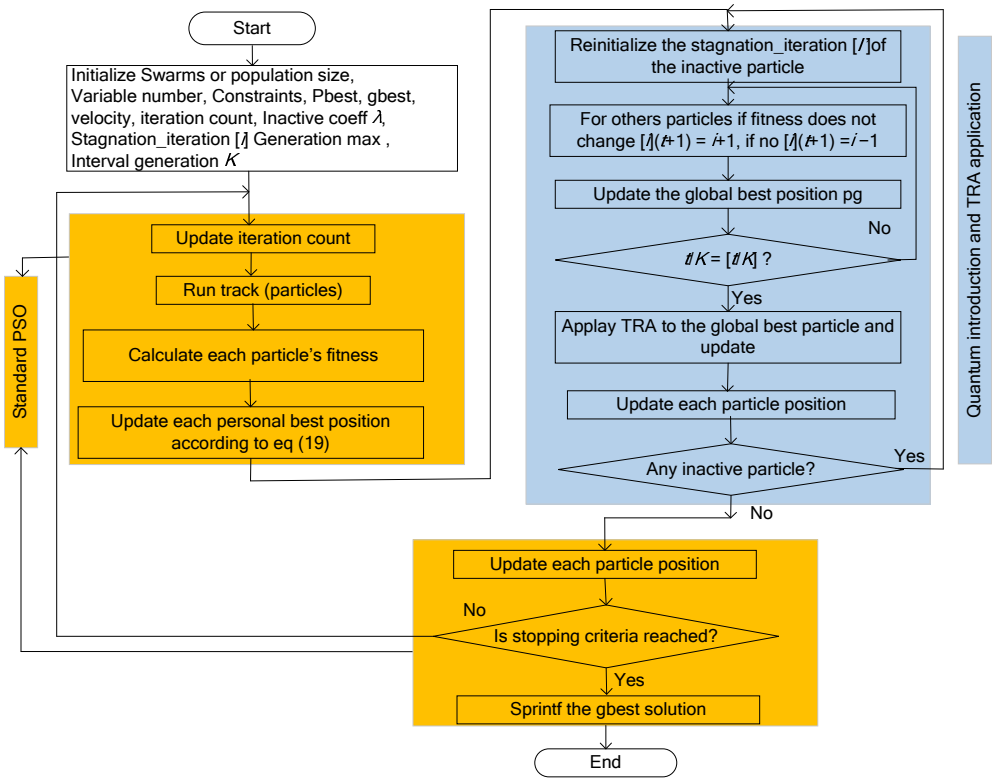

Figure 2. Flowchart of QPSO-TRA.

4. Experimental Validation

4.1. Laboratory Test

A Matlab program was made for the implementation to identify the parameters of a 5.5 kW, 380 V, 11.7 A, 1450 r/min, and design B induction motor using the proposed algorithm in the laboratory. Figure 3 depicts the test rig of 5.5 kW motor. The test was performed with a power analyzer, a torque transducer and visualizer, a data acquisition system, a DC generator as load, and an auto-transformer used for different voltage conditions. The motor was run at full-load condition to obtain its stable temperature, and the hot temperature was measured. The equivalent circuit parameters method was associated with the algorithm to estimate the motor parameters. The optimization of parameters identification of the induction motor was mathematically expressed as follows: find $X = (x_1, x_2, \ldots, x_n)$ such that $F(X)$ is a minimum. The following are the identification variables for the optimization (X): stator leakage reactance X_1; core resistance R_{fe}; core magnetization reactance X_m, and rotor resistance R_2. The rotor leakage reactance X_2 is calculated with the value of stator leakage reactance X_1, as shown in Table 2. Four parameters out of six will be determined using the QPSO-TRA algorithm, as cited above.

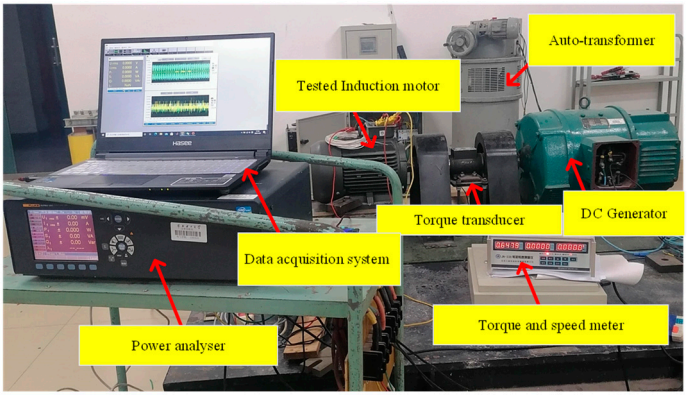

Figure 3. Test rig of 5.5 kW motor.

Table 2. Ratio of X_1/X_2 according to the design class [8].

Design Class	X_1/X_2
A	1.00
B	0.67
C	0.43
D	1.00
Wound rotor	1.00

Those four parameters represent the four variable particles in the QPSO-TRA algorithm. The algorithm needs one initial value, the value of stator resistance R_s. This value is measured at standstill and is corrected with temperature rise during the identification process. In addition, the values of $R_{s,cor}$, and X_2 were monitored during all the iterations to respect the algorithm's lower and upper bounds constraints. A stagnation_iteration coefficient [i] is used to monitor each particle's fitness value to record the particle's location change. If the fitness value of a particle X_i does not improve during an iteration, the stagnation_iteration [i] is extended by one, otherwise it is dropped by one. To consider a particle to be dormant or inactive, its stagnation_iteration [i] must respond to [i] $\geq \lambda$ and then has to be reinitialized to give it a chance to be a new candidate for the research. Reinitialization will assist the dormant particle in escaping from the local optimum and enhancing its search skills. The dormant coefficient is chosen by the user based on the research space, and also its value is determined by the problem's severity. The dormant coefficient λ was set to 0.95 in our case.

In the iteration process of the QPSO, the TRA technique is performed on the current global best particle at each iteration k. Considering the computing severity of TRA, this combined approach harnesses the experience and knowledge of each particle swarm during the iteration. In the implementation process, a beginning point α_0 and trust region radius r_0 are first specified. Then, using the iterative procedures, a series of points $\{\alpha_a\}$ is constructed to search for the ideal solution. At each iteration, a tiny region is created called the trust region, centered on the current iteration point. By dealing with a subproblem inside this region, a trial step k is determined. Next, an evaluation function is utilized to evaluate if the trial step should be accepted, and the trust region radius for the following iteration is determined. If the testing step is accepted, $\alpha_{(a+1)} = \alpha_a - \beta_a$; otherwise, $\alpha_{(a+1)} = \alpha_a$. If the trial stage is successful, the new radius will be enlarged or maintained. The trust region exclusively uses the problem's information and region knowledge. The ideal combination is depicted in Equation (25). Because the original QPSO-TRA method is an optimization technique for obtaining optimum values, it leads the particle to deviate from the subregional minimum value and returns the optimal values when the iteration ends, where the fitness

represents the objective function, $\{X_i\}$ is the function of parameters to be identified, $\beta = [K,\alpha]$, K is an integer in the interval [1,6], and $\alpha = 50$ is the population size for the optimization:

$$\begin{cases} fitness = \min_{\beta=[K,\alpha]}\{X_i\} \\ K = [1,6] \\ \alpha = 250 \end{cases} \quad (25)$$

As constraints, the values of each particle's lower and upper bounds are set. The lower bound (lb) and upper bound (ub) are set for the motor's parameters. In our case, the lower and upper bounds were set to lb = [0.00 0.00 0.00 0.00 0.00 0.00] and ub = [2.4.00 1.00 1.20 2853 155.00 5.50] for the six parameters of the motors, namely, stator resistance, stator reactance, rotor reactance, core resistance, magnetizing reactance, and rotor resistance, respectively. These lower and upper bounds depend on the size of the motors. Then, the algorithm runs until the stopping criterion is reached. After their identification by QPSO-TRA, $R_{s,cor}$ is used for air gap torque determination, and R_{fe} is used for core losses determination in the proposed efficiency estimation algorithm. The remaining parameters can be used to judge the motor winding healthy state.

The current signal is collected using a data acquisition system for the motor speed detection technique, as shown in Figure 4a. FFT was used to obtain the current frequency spectrum. All the frequency components in the spectrum cannot be directly used. A range of harmonic frequencies must be defined as a criterion for harmonics frequency determination. The number of the spectrum component is reduced by determining lower and upper threshold values, a range of probable frequencies for harmonics investigation. The high harmonics frequencies determine this range in no-load f_{sh1} and f_{sh2} in the full-load conditions. For example, suppose n_1, n_2, and z are, respectively, the synchronous speed (no-load speed), the rated speed, and the rotor slot number. In that case, the harmonic frequency is determined using the formulas $f_{sh1} = \frac{n_1 z}{60} \pm f_0$ and $f_{sh2} = \frac{n_2 z}{60} \pm f_0$, where f_0 is the supply frequency. The frequency components that are not in the range are eliminated to reduce or limit the research space. Then, those frequencies that are in the range are investigated to calculate the probable rotor slot harmonic frequency (RSHF). In our case, the determination range was 680–800 Hz. The frequency that has high amplitude is the identified slot harmonic frequency. Once the RSHF is obtained, Equation (5) is used to determine the motor speed. Figure 4b shows that the identified slot harmonic frequency is 734 Hz, and the speed is 1466 r/min. Figure 5a illustrates the estimated versus measured speed according to load ratio; whiles Figure 5b depicts estimated versus measured efficiency according to load ratio, which show a good agreement with the measured results.

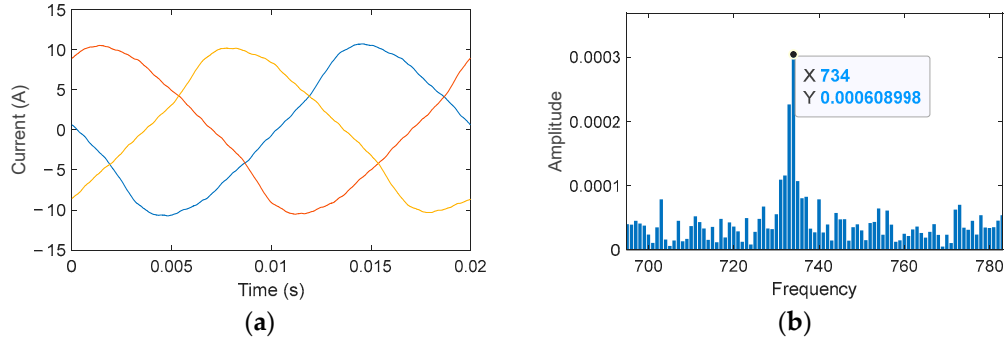

Figure 4. Measured stator current and rotor harmonic frequency: (**a**). measured phase-A currents; (**b**). extracted rotor slot harmonics frequency (734 Hz) for 5.5 kW motor, with slot number $Z = 28$ and pole pair number $p = 2$; the corresponding speed is 1465.71 r/min after recorded data analysis.

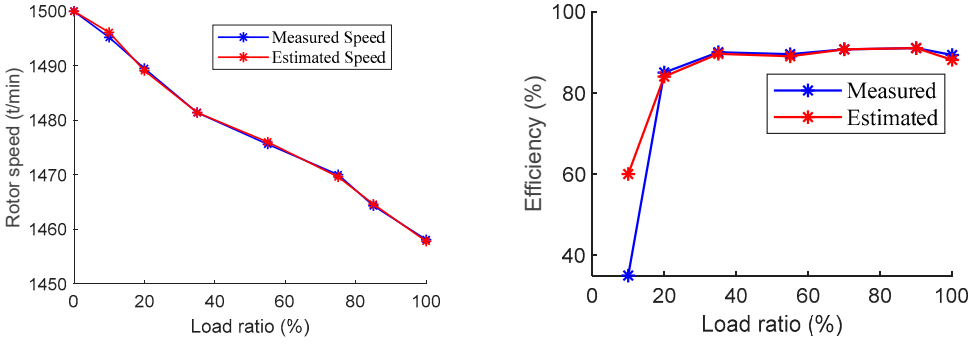

(**a**) (**b**)

Figure 5. Measured versus estimated: (**a**). estimated versus measured speed according to load ratio; (**b**). estimated versus measured efficiency according to load ratio.

Table 3 shows the extracted parameters and compares PSO and QPSO-TRA algorithms for motor parameters determination. The speed has also been measured using a contactless method and both results were compared to evaluate the speed detection technique. After the full load, partial loads such as 75%, 50%, and 25% were also tested. Table 4 depicts the motor measured efficiencies and their associated speeds. The full charge and partial loads results are shown in Table 4. The relative errors of both efficiencies and speed can also be seen. Table 4 also illustrates the estimated efficiencies with PSO and QPSO-TRA and the estimated speeds versus measured speeds of the partial loads in the laboratory. The relative error deviations of the estimated efficiencies from the measured values are presented. For comparison purposes, PSO and QPSO-TRA results are shown in Table 4 for a laboratory test.

Table 3. Comparison of determined parameters of 5.5 kW motor.

Parameters	PSO	QPSO-TRA
R_1	2.43	2.43
R_2	1.92	1.72
R_{fe}	2803.87	2687.675
X_m	114.15	150.003
X_1	0.88	0.85
X_2	1.31	1.27

Table 4. 5.5 kW motor estimated efficiencies and speeds versus measured in the laboratory.

Load (%)	Speeds (r/min)		Relative Errors	Efficiencies (%)			Relative Errors PSO/QPSO-TRA
	Measured	Estimated		Measured	Estimated		
					PSO	QPSO-TRA	
100	1468.04	1465.71	0.0158	88.63	91.05	89.32	0.1900
75	1475.08	1473.88	0.0081	91.41	90.94	91.65	−0.0780
50	1481.4	1482.5	−0.0007	90.04	89.55	89.95	−0.0446
25	1489.5	1490.8	−0.0008	83.86	89.33	83.53	0.6492

It is evident that the error increases with the load factor of 25%. At 25%, the motor is under light load condition. At this point, the losses are more considerable than if the load point is close to the rated load and the output power is small, which is not recommended because it is not beneficial.

4.2. Field Application

The proposed algorithm has been applied on an 11,000 kW, 10 kV feeding pump induction motor in a power plant, the rated current and speed are 710 A and 1491 rpm,

respectively. Figure 6 shows the measured voltage and current waveforms of the above motor. In the field test, a self-developed monitoring system is installed on the motor terminal, and the running interface is to complete the corresponding data monitoring and analysis. Besides of the voltage and current waveforms, the monitored data also include voltage, current, torque, speed, power factor, efficiency, voltage deviation, unbalance and harmonic components and so on. Here, when monitoring and recording a large amount of data, only a typical example of data is given in Figure 6 and Table 5. It can be seen that.

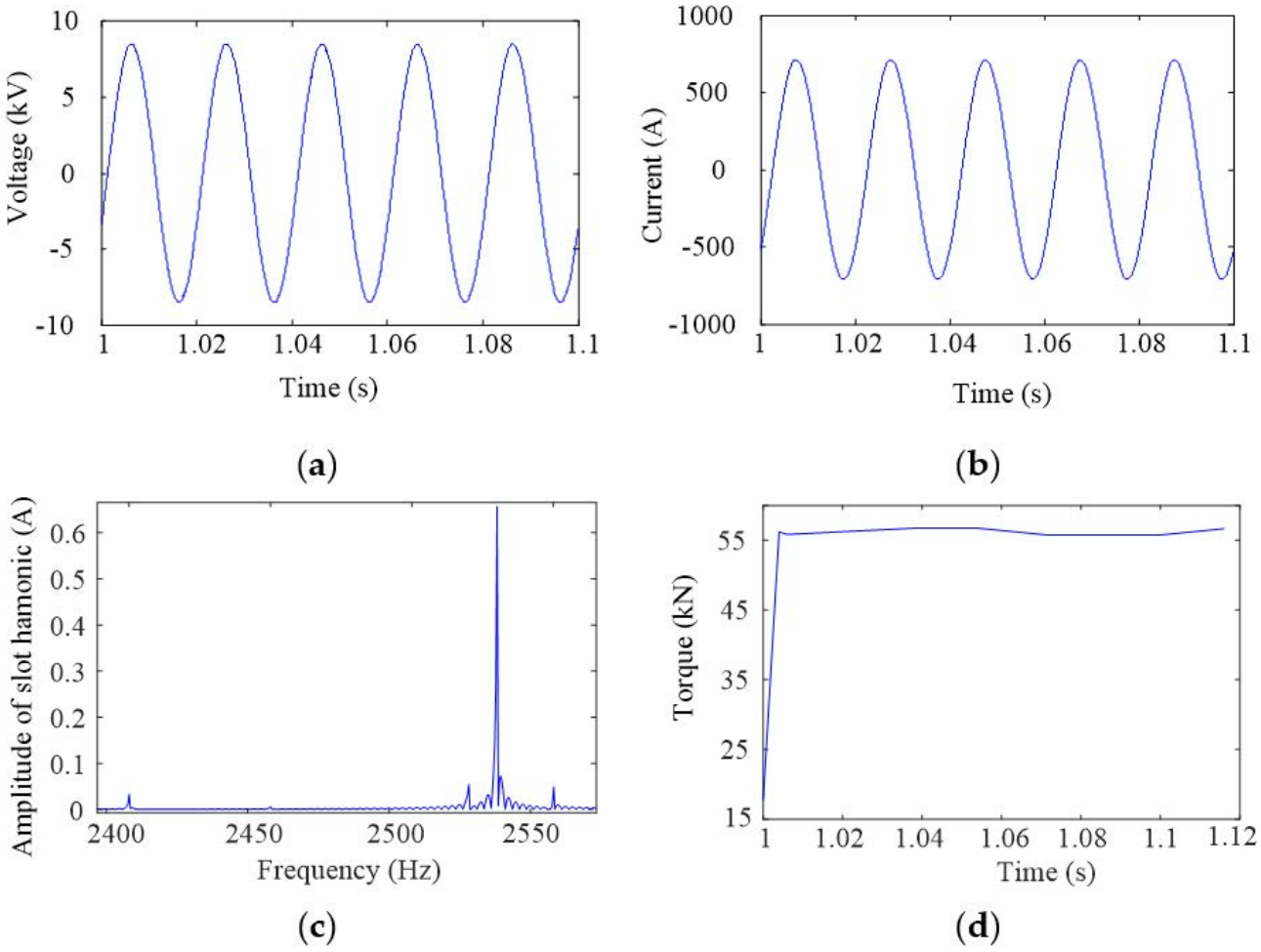

Figure 6. Measured waveforms with the developed monitoring system and estimated air-gap torque and slot harmonic obtained by the presented method. (**a**). Voltage. (**b**) Current. (**c**) Air-gap torque. (**d**) Rotor slot harmonic.

Table 5. Extracted parameters by QPSO-TRA and PSO.

Parameters	10 MW Motor	
	QPSO-TRA	PSO
R_1	0.223	0.351
R_2	0.172	0.272
R_{fe}	28,687.675	29,381.178
X_m	2350.003	2715.078
X_1	0.115	0.231
X_2	0.115	0.231

(1) Figure 6a,b are the measured voltage and current waveforms, and Figure 6c,d are identified rotor slot harmonics and electromagnetic torque. The input power can be

calculated by measured voltage and current waveforms, namely, 8922.27 kW. Furthermore, it is difficult to measure the shaft torque directly in the field, therefore, the output power are derived by the measured speed and pressure and flow of pumped water, namely, 8565.92 kW, respectively. And motor efficiency under this condition is 96.01%.

(2) From Figure 6c,d, the identified rotor slot harmonic is 2540 Hz, and the related rotor speed is 1494.5 rpm, and average electromagnetic torque under this condition based on Equation (2) is 55 kNm. It can be calculated that the output power is 8603.33 kW. And the identified efficiencies are 95.63% and 96.43%, with PSO and QPSO-TRA, respectively.

(3) Table 5 shows the extracted parameters of the motor using QPSO-TRA and PSO algorithms, respectively. Table 6 shows the motor data and the estimation results. It can be concluded that the estimated results show that the relative error is about 0.83% in the field test, which indicates that the proposed method can meet the efficiency estimation requirement of motor systems.

Table 6. Measured versus estimated efficiencies of the motors by PSO and QPSO-TRA methods.

Measured Efficiency (%)	Estimated Efficiency by PSO (%)	Estimated Efficiency QPSO-TRA (%)	Relative Errors PSO/QPSO-TRA
96.01	95.63	96.43	0.83

To sum up, the proposed algorithm demonstrates an sufficient accuracy level when the predicted or estimated efficiencies are compared to their related measured values.

5. Conclusions

This study proposes an approach for in situ efficiency estimation of induction motors based on the QPSO-TRA algorithm. With the proposed method, the stator resistance R_s and the core losses resistance R_{fe} can be accurately identified online. The main conclusions are as follows.

(1) A new algorithm to identify the motor parameters is designed to deal with the problem mentioned early for induction motor parameters identification. This new algorithm is called QPSO-TRA. After comparing the extracted parameters with QPSO-TRA and standard PSO, it is found that QPSO-TRA can achieve a better result than the standard PSO, as can be seen in Tables 3 and 5.

(2) With the proposed hybrid algorithm, global research is avoided when investigating the full research space. The computation time and burden are reduced to 1/3 compared to the Genetic Algorithm and also the algorithm is faster, reducing the computational time, compared to simple TRA.

(3) Experiments in the laboratory and the field were performed to analyze the performance of the proposed efficiency estimation algorithm by testing some induction motors of various types and rating power in the laboratory rather than in the field. The relative errors in Tables 4 and 6 are less than 2%, which is a good indicator to show the high accuracy of the proposed method. Finally, the high accuracy level showed by the proposed technique validated the efficiency estimation technique.

Author Contributions: Methodology—M.N.D. and Y.Y.; Conceptualization—Y.L. and H.Z.; Validation, M.N.; Data analysis, M.N.D., Y.Y., and H.Z.; writing—original draft preparation, M.N.D., Y.Y. and Z.L.; writing—review and editing, H.Z.; supervision, Y.L. and H.Z. All authors have read and agreed to the published version of the manuscript.

Funding: This research was funded by the National Natural Science Foundation of China under Grant No. 52177041.

Institutional Review Board Statement: Not applicable.

Informed Consent Statement: Not applicable.

Data Availability Statement: Not applicable.

Acknowledgments: The authors would like to thank SOACAP-MALI (Société Africaine de Chaussures et Articles en Plastiques: African Company for Shoes and Plastic Products) for their support which helped to improve the outcome feasibility of the research.

Conflicts of Interest: The authors declare no conflict of interest.

References

1. Gajjar, C.S.; Kinyua, J.M.; Khan, M.A.; Barendse, P.S. Analysis of a Nonintrusive Efficiency Estimation Technique for Induction Machines Compared to the IEEE 112B and IEC 34-2-1 Standards. *IEEE Trans. Ind. Appl.* **2015**, *51*, 4541–4553. [CrossRef]
2. Esen, G.K.; Ozdemir, E. A New Field Test Method for Determining Energy Efficiency of Induction Motor. *IEEE Trans. Instrum. Meas.* **2017**, *66*, 3170–3179. [CrossRef]
3. Santos, V.S.; Eras, J.J.C.; Gutierrez, A.S.; Ulloa, M.J.C. Assessment of the energy efficiency estimation methods on induction motors considering real-time monitoring. *Energy Convers. Manag.* **2019**, *136*, 237–2470. [CrossRef]
4. Al-Badri, M.; Pillay, P.; Angers, P. A Novel In Situ Efficiency Estimation Algorithm for Three-Phase IM Using GA, IEEE Method F1 Calculations, and Pretested Motor Data. *IEEE Trans. Energy Convers.* **2015**, *30*, 1092–1102. [CrossRef]
5. Hsu, J.S.; Sorenson, P.L. Field Assessment of Induction Motor Efficiency through Air-Gap Torque. *IEEE Trans. Energy Convers.* **1996**, *11*, 489–494. [CrossRef]
6. Bijan, M.G.; Al-Badri, M.; Pillay, P.; Angers, P. Induction Machine Parameter Range Constraints in Genetic Algorithm Based Efficiency Estimation Techniques. *IEEE Trans. Ind. Appl.* **2018**, *54*, 4186–4197. [CrossRef]
7. Siraki, G.; Pillay, P. An in situ efficiency estimation technique for induction machines working with unbalanced supplies. *IEEE Trans. Energy Convers.* **2012**, *27*, 85–95. [CrossRef]
8. *Std 112-2004 (Revision IEEE Std 112-1996)*; IEEE Standard Test Procedure for Polyphase Induction Motors and Generators 2004. IEEE Press: Piscataway, NJ, USA, 2018; pp. 1–83.
9. Hsu, J.; Scoggins, B. Field test of motor efficiency and load changes through air-gap torque. *IEEE Trans. Energy Convers.* **1995**, *10*, 477–483. [CrossRef]
10. Santos, V.S.; Felipe, P.R.V.; Sarduy, J.R.G.; Lemozy, N.A.; Jurado, A.; Quispe, E.C. Procedure for Determining Induction Motor Efficiency Working Under Distorted Grid Voltages. *IEEE Trans. Energy Convers.* **2015**, *30*, 331–339. [CrossRef]
11. Siraki, A.G.; Pillay, P.; Angers, P. Full Load Efficiency Estimation of Refurbished Induction Machines from No-Load Testing. *IEEE Trans. Energy Convers.* **2013**, *28*, 317–326. [CrossRef]
12. Siraki, G.; Pillay, P. Comparison of two methods for full-load in situ induction motor efficiency estimation from field testing in the presence of over/undervoltages and unbalanced supplies. *IEEE Trans. Ind. Appl.* **2012**, *48*, 1911–1921. [CrossRef]
13. Desai, C.; Pillay, P. Back EMF, torque-angle, and core loss characterization of a variable-flux permanent-magnet machine. *IEEE Trans. Transp. Electrif.* **2019**, *5*, 371–384. [CrossRef]
14. Zhang, Z.; Deng, Z.; Sun, Q.; Peng, C.; Gu, Y.; Pang, G. Analytical Modeling and Experimental Validation of Rotor Harmonic Eddy-Current Loss in High-Speed Surface-Mounted Permanent Magnet Motors. *IEEE Trans. Magn.* **2018**, *55*, 100811. [CrossRef]
15. Climente-Alarcon, V.; Antonino-Daviu, J.A.; Haavisto, A.; Arkkio, A. Diagnosis of Induction Motors Under Varying Speed Operation by Principal Slot Harmonic Tracking. *IEEE Trans. Ind. Appl.* **2015**, *51*, 3591–3599. [CrossRef]
16. Silva, W.L.; Lima, A.M.N.; Oliveira, A. Speed Estimation of an Induction Motor Operating in the Nonstationary Mode by Using Rotor Slot Harmonics. *IEEE Trans. Instrum. Meas.* **2014**, *64*, 984–994. [CrossRef]
17. Al-Badri, M.; Pillay, P.; Angers, P. A Novel in Situ Efficiency Estimation Algorithm for Three-Phase Induction Motors Operating with Distorted Unbalanced Voltages. *IEEE Trans. Ind. Appl.* **2017**, *53*, 5338–5347. [CrossRef]
18. Stopa, M.M.; Resende, M.R.; Luiz, A.S.A.; Justino, J.C.G.; Rodrigues, G.G.; Filho, B.J.C. A Simple Torque Estimator for In-Service Efficiency Determination of Inverter-Fed Induction Motors. *IEEE Trans. Ind. Appl.* **2020**, *56*, 2087–2096. [CrossRef]
19. Salomon, C.P.; Sant'Ana, W.C.; da Silva, L.E.B.; Lambert-Torres, G.; Bonaldi, E.L.; de Oliveira, L.E.L.; da Silva, J.G.B. Induction Motor Efficiency Evaluation Using a New Concept of Stator Resistance. *IEEE Trans. Instrum. Meas.* **2015**, *64*, 2908–2917. [CrossRef]
20. Bramerdorfer, G.; Tapia, J.A.; Pyrhonen, J.J.; Cavagnino, A. Modern Electrical Machine Design Optimization: Techniques, Trends, and Best Practices. *IEEE Trans. Ind. Electron.* **2018**, *65*, 7672–7684. [CrossRef]
21. Wang, P.-P.; Chen, X.-X.; Zhang, Y.; Hu, Y.-J.; Miao, C.-X. IBPSO-Based MUSIC Algorithm for Broken Rotor Bars Fault Detection of Induction Motors. *Chin. J. Mech. Eng.* **2018**, *31*, 80. [CrossRef]
22. Liu, F.; Gao, J.; Liu, H. A Fault Diagnosis Solution of Rolling Bearing Based on MEEMD and QPSO-LSSVM. *IEEE Access* **2020**, *8*, 101476–101488. [CrossRef]
23. Hu, C.; Reeves, S.J. Trust Region Methods for the Estimation of a Complex Exponential Decay Model in MRI With a Single-Shot or Multi-Shot Trajectory. *IEEE Trans. Image Process.* **2015**, *24*, 3694–3706. [PubMed]